

## Analysis of cartilage matrix fixed charge density and three-dimensional morphology via contrast-enhanced micro-computed tomography

Ashley W. Palmer, Robert E. Guldberg, and Marc E. Levenston  
Georgia Institute of Technology  
Atlanta, U.S.A.

### Customer need

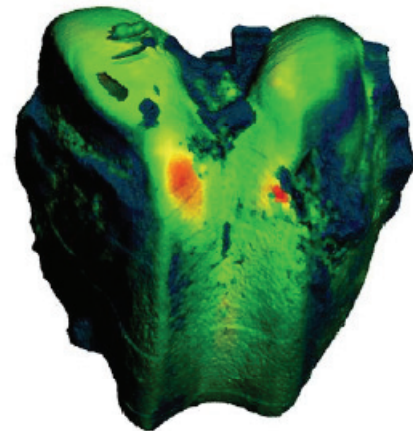
Small animal models of osteoarthritis are often used for evaluating the efficacy of pharmacologic treatments and cartilage repair strategies, but non-invasive techniques capable of monitoring matrix-level changes are limited by the joint size and the low radiopacity of soft tissues.

Here we present a technique for the non-invasive imaging of cartilage at micrometer-level resolution based on detecting the Equilibrium Partitioning of an Ionic Contrast-agent via  $\mu$ -Computed Tomography (EPIC- $\mu$ CT). The approach exploits electrochemical interactions between the molecular charges present in the cartilage matrix (ECM) and an ionic contrast agent, resulting in a non-uniform equilibrium partitioning of the ionic contrast agent reflecting the proteoglycan (PG) distribution.

In an in vitro model of cartilage degeneration we observed changes in x-ray attenuation magnitude and distribution consistent with biochemical and

histological analyses of sulphated glycosaminoglycans (sGAGs), and x-ray attenuation was found to be a strong predictor of sGAG density. Equilibration with the contrast agent also permits direct in situ visualization and quantification of cartilage surface morphology.

Equilibrium partitioning of an ionic contrast agent via micro-computed tomography thus provides a powerful approach to quantitatively assess 3D cartilage composition and morphology for studies of cartilage degradation and repair.



0.000mm  0.720mm

Fig. 1. Thickness map generated after segmentation of soft tissue and bone.

### Customer need

Non-invasive imaging of cartilage and a quantitative assessment of the 3D cartilage composition and morphology.

### Materials and methods

SCANCO Medical  $\mu$ CT 40 and vivaCT 40 scanner were used together with equilibrium partitioning of an ionic contrast agent (EPIC) to produce the images.

### Results

This work details the development of EPIC- $\mu$ CT, a technique for the 3D, quantitative imaging of proteoglycan distributions in soft tissues. EPIC- $\mu$ CT also shows the ability to produce 3D images of the articular surface of cartilage in situ.

### Materials and methods

**Principle of the Technique:** Similar to the dGEMRIC technique, EPIC-  $\mu$ CT relies on the partitioning of a charged contrast agent within a charged ECM. In cartilage, type II collagen carries a nearly neutral net charge whereas the sulphated GAGs primarily associated with the large, aggregating PG can confer a highly negative net charge to the ECM. The interstitial fluid carries a corresponding excess of positively charged solutes, resulting in bulk macroscopic electro neutrality. Given these

properties, conditions of electrochemical equilibrium predict that a negatively charged solute capable of permeating the tissue would distribute inversely to the negatively charged sGAGs and therefore spatially target regions of lower sGAG density. For a region of tissue with a Fixed Charge Density (FCD)  $\rho_m$  (in Coulombs/litre) submerged in a bath containing a single monovalent salt at a concentration  $C_o$ , the Gibbs–Donnan theory for an ideal solution predicts the interstitial anion concentration within the tissue  $C^*$  as:

$$C^* = \frac{-\rho_m + \sqrt{\rho_m^2 + (2FC_o)^2}}{2F} \quad [1],$$

where  $F$  is Faraday’s constant. For a tissue such as cartilage, a negatively charged solute capable of permeating the tissue would distribute inversely to the negatively charged sGAGs and therefore spatially target regions of lower sGAG density. If the anion concentration could be noninvasively detected it would thus provide an indirect measure of the matrix FCD (and therefore the sGAG concentration).

It should be noted that although Eq. 1 describes the distribution of an ideal anionic solute in a dilute solution, there are in practice several other factors which result in deviations from the ideal behaviour. See the original publication (1) for a more exact description.

Also in that publication a detailed description of the methods used to validate EPIC- $\mu$ CT can be found. These are:

1. The usage of in vitro evaluation.
2. Tissue explants preparation and culture.
3.  $\mu$ CT scanning and analysis (Scanco Medical vivaCT 40).
4. Biochemical analysis.
5. Histology.
6. In situ imaging of Rabbit Femur.

## Results

3D images obtained from EPIC- $\mu$ CT scanning were used to visualize the sGAG distribution in full-thickness control and IL-1-stimulated explants (Fig. 2). Consistent with the assumed inverse partitioning of the negatively charged ioxaglate dimer within the ECM of cartilage, low x-ray attenuation corresponded to regions of high sGAG content and high x-ray attenuation indicated regions of low sGAG content. Control explants showed little visible variation in x-ray attenuation with culture time. In contrast, increases in x-ray attenuation were

apparent for IL-1-stimulated explants beginning at day 4. In our full-thickness explant model, increases in x-ray attenuation appeared first in the superficial zone, in the deep zone, and on the outer surfaces of the IL-1-stimulated explants and progressed toward the interior with time.

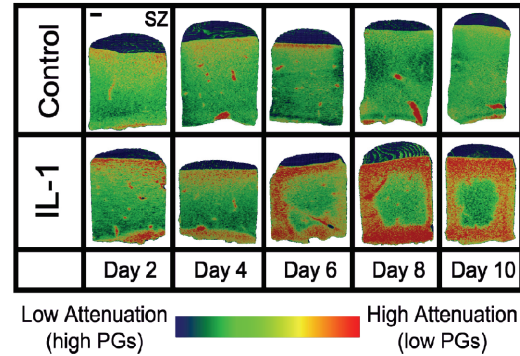


Fig. 2. In Vitro Cartilage Degeneration Model: EPIC- $\mu$ CT Images.

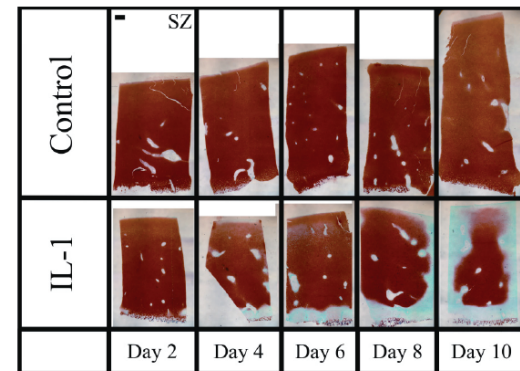


Fig. 3. In Vitro Cartilage Degeneration Model: Safranin-O staining Histology.

Histological sections revealed similar patterns of sGAG depletion. In longitudinal sections taken from the centre of full-thickness explants, control explants exhibited a dense, uniform distribution of sGAGs (Fig. 3). In contrast, IL-1-stimulated explants exhibited visible decreases in sGAG staining beginning at day 4 and continuing throughout the culture period. The decreased staining in the IL-1 group consistently progressed from the superficial zone, the deep zone, and the outer surfaces inward, consistent with the locations of increased attenuation in the EPIC- $\mu$ CT images.

Consistent with the EPIC- $\mu$ CT and histology images, the overall average x-ray attenuation for the full-thickness control explants did not significantly vary with culture time (Fig. 4). In contrast, the attenuation of IL-1-stimulated explants progressively increased, with levels significantly higher than in control explants beginning at day 6.

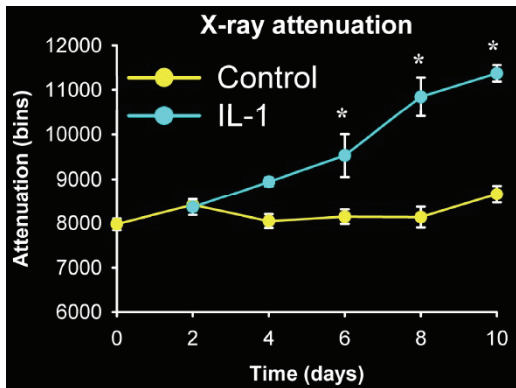


Fig. 4. In Vitro Cartilage Degeneration Model: Quantitative Changes in PG Content.

Consistent with the EPIC- $\mu$ CT and histology images, the overall average x-ray attenuation for the full-thickness control explants did not significantly vary with culture time (Fig. 4). In contrast, the attenuation of IL-1-stimulated explants progressively increased, with levels significantly higher than in control explants beginning at day 6.

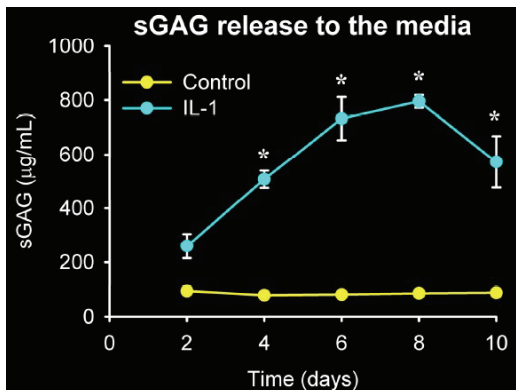


Fig. 5. IL-1 stimulation results in progressive loss of sGAGs with time by histology and DMMB assay

The increased release of PGs to the media in response to IL-1 treatment was consistent with the increase in x-ray attenuation. Full-thickness control explants released a low level of sGAGs throughout the 10-day culture (Fig. 5). In contrast, IL-1-stimulated cartilage showed a characteristic rise in media sGAG levels that peaked at day 8 and was significantly elevated over control explants beginning at day 4. The progressive loss of sGAGs to the media was consistent with both reduced Safranin-O staining and increased attenuation in EPIC- $\mu$ CT analysis.

To directly examine the relationship between explant composition and x-ray attenuation, both control and IL-1-stimulated cartilage explants were digested and analyzed for sGAG content after EPIC- $\mu$ CT scanning. A linear regression analysis revealed a significant relationship ( $r^2=0.91$ ,  $P < 0.0005$ ) between

x-ray attenuation and sGAG/H<sub>2</sub>O (Fig. 6). The negative Pearson coefficient,  $r = -0.95$ , agreed with the assumed inverse distribution of a negatively charged contrast agent and sGAGs within the ECM.

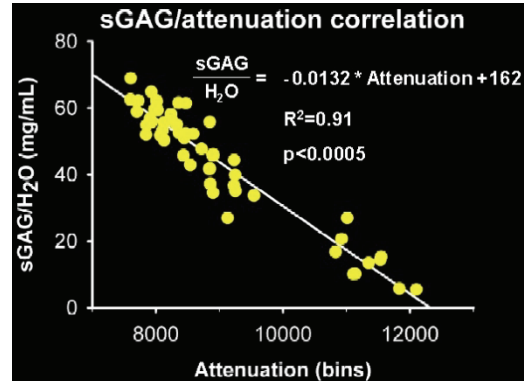


Fig. 6. Correlation of X-Ray Attenuation and sGAG Concentration.

## Rabbit Articular Cartilage Imaging

Fig. 7 is a photograph of the actual distal femur. The reconstructed image of an immature rabbit femur after exposure to a 40%/60% solution of Hexabrix/0.15 M PBS reveals articular surface topography and soft tissue features (Fig. 8). In particular, the EPIC- $\mu$ CT images demonstrate the ability to distinguish ligament insertion points (black arrows) and a scalpel mark on the articular surface (white arrow). After segmentation of cartilage from bone using thresholds identified from the histogram, a thickness map of the articular cartilage surface layer (Fig. 1) indicates thickness values that are consistent with the anticipated regional variations in rabbit articular cartilage thickness.

## Discussion

Non-invasive techniques capable of detecting PG content and distribution and tissue morphology could dramatically improve upon existing evaluation options for monitoring the efficacy of OA treatments and cartilage repair strategies. This work details the development of EPIC- $\mu$ CT, a technique for the 3D, quantitative imaging of PGs in soft tissues. By using IL-1 stimulation of articular cartilage as an in vitro degradation model, the ability of EPIC- $\mu$ CT to monitor the progressive loss of sGAGs from cartilage explants was demonstrated. In addition, the strong correlation found between x-ray attenuation and sGAG density indicates that this technique can be used not only to monitor relative changes in sGAG content and distribution, but also to quantitatively evaluate sGAG content, a feature that may prove useful for in vitro analysis of matrix changes in

studies of tissue degeneration and development of tissue engineered constructs.

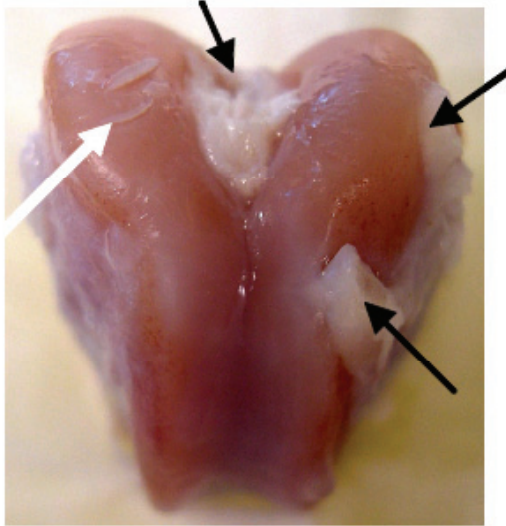


Fig. 7. Rabbit distal femur

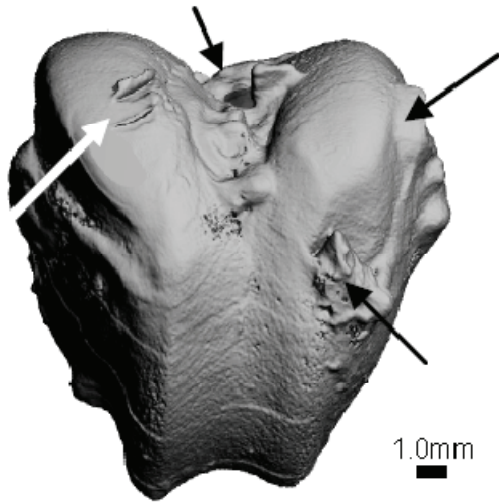


Fig. 8. In situ EPIC-μCT imaging of Rabbit distal femur

EPIC-μCT also shows the ability to produce 3D images of the articular surface of cartilage in situ, illustrating potential applications in monitoring surface contours and engineered construct integration in defect repair studies as well as regional variations in cartilage thickness. The EPIC-μCT technique is complementary to several other methods that have recently been introduced (see ref. 2 to 6). Although these referenced methods provide high-resolution planar images, quantitative analyses of 3D distributions and morphology are not currently possible. Although it is not currently viable as a clinical imaging modality, the ability to simultaneously provide quantitative data regarding

tissue composition and morphology makes EPIC-μCT a powerful research tool.

With the non-invasive, high-resolution monitoring capability of μCT, the greatest benefit of this technique may lie in the assessment of ECM changes in rodent models of cartilage degeneration and regeneration. A promising extension of this work is the application of EPIC-μCT for end-stage analysis of intact cartilage surfaces after dissection of small-animal joints.

Furthermore, the capability of commercial μCT scanners for in vivo analysis raises the exciting possibility of longitudinal monitoring of cartilage matrix changes during disease or treatment progression in individual animals.

Some critical steps in advancing this technique still have to be made (see ref. 1 for details). However, despite these potential limitations, the present study establishes the basis for a quantitative, high resolution, 3D imaging technique capable of non-destructively monitoring cartilage matrix organization in vitro that may become a powerful tool for analyzing small-animal models of cartilage degeneration and regeneration.

## References

1. Palmer AW et al. (2006) in *PNAS*, vol. 103, no. 51, p19255-19260.
2. Bashir A, et al. (1996) in *Magn Reson Med* 36: 665-673
3. Kim YJ, et al. in *J Bone Joint Surg Am* 85-A: 1987-1992
4. Cockman MD, et al. (2006) in *Osteoarthritis Cartilage* 14:210-214.
5. Patel NA et al. (2005) in *IEEE Trans Med Imaging* 24:155-159.
6. Camacho NP, et al. (2001) in *Biopolymers* 62:1-8

### SCANCO equipment

SCANCO Medical μCT 40 and a vivaCT 40 scanner

### SCANCO software

Measurement program incl. Scout View  
Evaluation program

- ✓ Segmentation
- ✓ 2D/3D morphometric analysis
- ✓ Density measurement

Visualization program